Abruptly autofocusing waves

Nikolaos K. Efremidis[1,*] and Demetrios N. Christodoulides[2]

[1]*Department of Applied Mathematics, University of Crete, 71409 Heraklion, Crete, Greece*

[2]*CREOL/College of Optics, University of Central Florida, Orlando, Florida 32816, USA*

**Corresponding author: nefrem@tem.uoc.gr*

Received August 26, 2010; revised October 18, 2010; accepted October 24, 2010;
posted November 9, 2010 (Doc. ID 133783); published November 29, 2010

We introduce a new class of $(2+1)$D spatial and $(3+1)$D spatiotemporal waves that tend to autofocus in an abrupt fashion. While the maximum intensity of such a radial wave remains almost constant during propagation, it suddenly increases by orders of magnitude right before its focal point. These waves can be generated through the use of radially symmetric Airy waves or by appropriately superimposing Airy wave packets. Possible applications of such abruptly focusing beams are also discussed.

OCIS codes: 050.1940, 260.2030, 350.5500.

The focusing characteristics of optical beams have always been an issue of great practical importance [1]. In general, a wave tends to focus or defocus whenever its initial phase and/or amplitude have been suitably manipulated. In the case of a Gaussian wavefront—perhaps the most prevalent of all beams—the peak intensity follows a Lorentzian distribution around the focus or minimum waist point. Their corresponding higher-order modes (Hermite– or Laguerre–Gaussian) also behave in a similar manner [1,2]. On the other hand, the respective behavior of other families of waves can be considerably more involved, especially close to the focus.

For many applications it is crucial that a beam abruptly focuses its energy right before a target while maintaining a low intensity profile until that very moment. Ideally, this should be a linear property of the wave itself and not the outcome of any self-focusing effects [2]. In medical laser treatments this feature may be highly desirable, since the wave should only affect the intended area while leaving any preceding tissue intact [3]. In several experimental settings, such behavior can also be useful in suddenly "igniting" a particular nonlinear process, such as multiphoton absorption, stimulated Raman, and optical filaments in gases, locally only after the focus [4–7]. This will ensure that no energy is nonlinearly lost due to gradual focusing effects, for example, as is the case of Gaussian beams. To realize this fascinating prospect, it is, therefore, important to identify a new class of optical beams for which the internal energy flux tends to accumulate at the focus in an accelerated manner during propagation.

In this Letter, we introduce new families of radially symmetric (cylindrical and spherical) waves with this desired characteristic: their maximum intensity remains almost constant during propagation, while close to a particular focal point, they suddenly autofocus and, as a result, their peak intensity can increase by orders of magnitude. In two dimensions, we present two different classes of such waves, which are based on a radial Airy profile and a superposition of two-dimensional Airy wave packets. In three dimensions, the spatiotemporal problem is exactly solved in the region of anomalous dispersion. In this latter case, even higher intensity contrasts are expected.

Let us start by considering the diffraction of a radially symmetric beam (i.e., a beam that in cylindrical spatial coordinates depends only on r and z) propagating in a linear medium. In the paraxial approximation, the beam dynamics satisfy

$$u_z = (i/2)(u_{xx} + u_{yy}) = (i/2)(u_r/r + u_{rr}), \tag{1}$$

where u is the amplitude of the optical wave, x, y are the scaled transverse coordinates, and z is the propagation distance normalized in Rayleigh lengths. For a given value of the wavelength, it depends on the spatial normalization factor x_0 whether paraxiality is satisfied. The propagation of an arbitrary radially symmetric initial condition $u(r, z=0) = u_0(r)$ can be computed in terms of the following Hankel transform pair:

$$u(r,z) = \frac{1}{2\pi}\int_0^\infty \mathrm{d}k k\tilde{u}_0(k) J_0(kr) e^{-ik^2 z/2}, \tag{2}$$

$$\tilde{u}_0(k) = 2\pi \int_0^\infty \mathrm{d}r r u_0(r) J_0(kr). \tag{3}$$

In the one-dimensional limit, Eq. (1) is known to support the following accelerating Airy beam [8,9]:

$$g(x,z) = \mathrm{Ai}(x - z^2/4 + i\alpha z)\exp[i(6\alpha^2 z - 6i\alpha(2x - z^2) + 6xz - z^3)/12]. \tag{4}$$

In Eq. (4), the decay parameter α ensures that the wave conveys finite energy (is thus realizable) and is typically small, so that the behavior of this wave approximates in many respects [8,9] that of an ideal ($\alpha = 0$) diffraction-free Airy wave packet [10]. Perhaps the most intriguing feature of this solution is its lateral parabolic acceleration.

Let us analyze the dynamics of radially symmetric Airy beams of the form $u_0(r) = \mathrm{Ai}(r_0 - r)\exp[\alpha(r_0 - r)]$, where r_0 is the initial radius of the main ring. For $r < r_0$, the Airy beam decays exponentially, whereas the slowly decaying oscillations of the Airy tails occur outside this region. The power that the Airy beam carries is given by $P = 2\pi\int_0^\infty |u_0(r)|^2 r\mathrm{d}r = \sqrt{\pi/(2\alpha)}e^{2\alpha^3/3}[r_0 + (1 - 4\alpha^3)/(4\alpha)]$. In the computation of the above integral, we extended the lower limit of integration from zero to minus infinity. Note that

this approximation does not affect the value of the integral, even for relatively small values of r_0, due to the exponential decay of the solution.

In Fig. 1(a), the amplitude of this cylindrical Airy beam is depicted as a function of z. If r_0 is large enough, then, during the initial stages of propagation, all the power is essentially located far from the center. As a result, the first term on the right-hand side of Eq. (1) is not significant, i.e., $\nabla_\perp^2 u \approx u_{rr}$. Thus, Eq. (4), with $x \to r_0 - r$, can approximate the radial dynamics. From Eq. (4), one may expect that the maximum value of the amplitude is going to slowly decrease along z. On the other hand, as z increases, the radius of the Airy beam decreases, the power concentrates in a smaller area, and thus the maximum amplitude increases. In fact, our simulations show that these two effects almost balance each other, leading to relatively small maximum amplitude changes, up to the point where the beam reaches the center [Figs. 1(a) and 1(b)]. Close to the focal point, the power of the first Airy ring is concentrated in a small area around $r = 0$ and the maximum intensity at the center rapidly increases. What is behind this very abrupt increase in intensity is the lateral acceleration of the Airy beams themselves. In this case, large transverse velocities are attained and energy rushes in an accelerated fashion toward the focus. This feature is unique to this family of waves. While the peak intensity remains around unity up to $z \approx 6$, it then very rapidly increases by more than 135 times at the focal point [Fig. 1(b)]. For longer propagation distances, the maximum intensity starts to decrease. As can be seen in Fig. 1(b), this decrease is not monotonic, but it exhibits oscillations, which are generated by the subsequent Airy rings.

In Fig. 1(c), the maximum intensity that the beam reaches during propagation is shown as a function of the initial radius r_0 for $\alpha = 0.05$. For small values of r_0, the Airy beam does not carry much power and thus the maximum intensity reached is also relatively small. As the value of r_0 increases, the maximum intensity also increases and for $r_0 \approx 15$ it takes its maximum value ($I_{\max} \approx 156$). For even larger values of r_0, diffraction becomes significant and $I_{\max}$ starts to decrease. Note that, as shown in Fig. 1(c), large intensity contrasts are possible for a wide range of values of r_0. Much higher values of $I_{\max}$ are possible by further suppressing diffraction (decreasing α). Figure 1(d) depicts the Hankel transform of the input field profile of this beam as a function of the radial spectral component k. The transform is a real function of k that oscillates between positive and negative values and its envelope is decreasing with k. Experimentally, such Airy beams in the Fourier space might be implemented by using the amplitude and phase masks shown in Fig. 1(d).

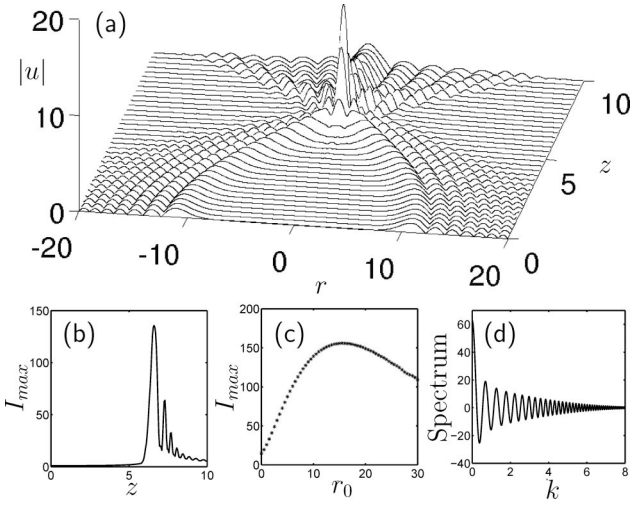

Fig. 1. Dynamics of radially symmetric Airy beams for $\alpha = 0.05$, $r_0 = 10$, and $I_{\max}(z = 0) = 1$. (a) Detailed plot of the central part of the propagation dynamics. (b) Maximum intensity as a function of z. (c) Maximum intensity that the Airy beam reaches during propagation for different values of the initial radius r_0. (d) Hankel transform of the initial condition as given by Eq. (3).

Particularly engineered superpositions of Airy functions can exhibit enhanced properties as compared to radially symmetric Airy beams. Here we introduce the transformations $x'(r,r_0,\theta_0) = r\cos(\theta_0) + r_0\sqrt{2}/2$, $y'(r, r_0, \theta_0) = -r\sin(\theta_0) + r_0\sqrt{2}/2$, which are used to define the following radially symmetric superposition of two-dimensional Airy beams:

$$u(r, r_0, z) = \int_0^{2\pi} g(x'(r, r_0, \theta_0), z) g(y'(r, r_0, \theta_0), z) \mathrm{d}\theta_0, \quad (5)$$

where $g(x, z)$ is given by Eq. (4). By setting $r = 0$ in Eq. (5), the amplitude profile is exactly computed at the center $u(r = 0, r_0, z) = 2\pi g^2(\sqrt{2}r_0/2, z)$. Notice that the intensity at the center is abruptly increasing as the fourth power of an Airy function with a complex argument. In Fig. 2, dynamical properties of such solutions are depicted. In comparison with Fig. 1 we notice two main differences: (a) the intensity contrasts achieved are larger [Fig. 2(c) versus Fig. 1(c)] and (b) the maximum intensities of the subsequent oscillations are smaller [Fig. 2(b) versus Fig. 1(b)]. We note that these beams represent a continuous superposition of Airy waves—in contrast to discrete sums recently used in clearing colloidal suspensions [11].

Three-dimensional spherically symmetric abruptly autofocusing waves are also possible in the region of

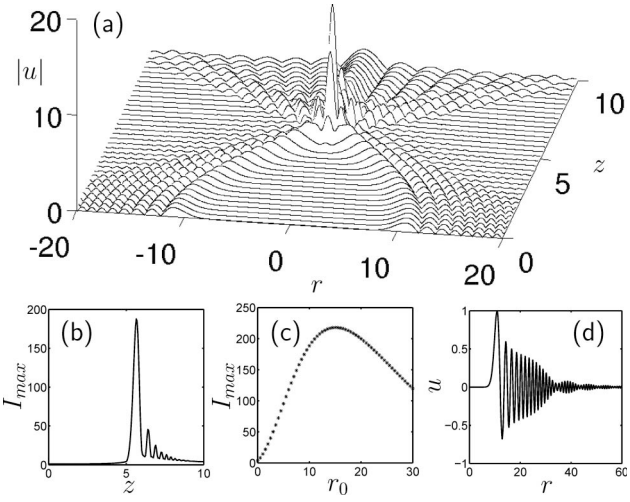

Fig. 2. Dynamics of the two-dimensional Airy superposition given by Eq. (5) for $\alpha = 0.05$, $r_0 = 10$, and $I_{\max}(z = 0) = 1$. (a), (b), (c) Same as in Fig. 1. (d) Amplitude of the solution.

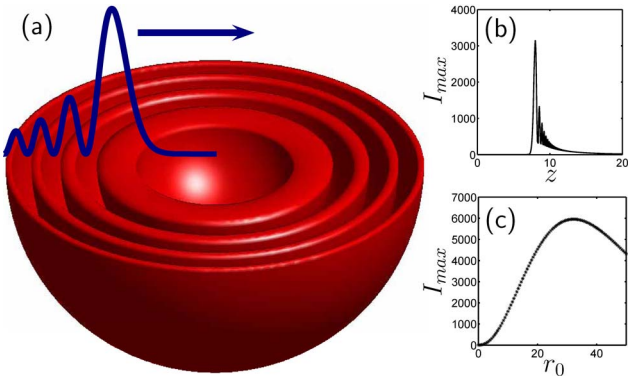

Fig. 3. (Color online) (a) Isointensity hemisphere of the Airy wave. (b), (c) Same as in Fig. 1 for the three-dimensional Airy solution given by Eq. (7) for $\alpha = 0.05$, $r_0 = 15$, and $I_{\max}(z = 0) = 1$.

anomalous dispersion, provided that dispersion and diffraction effects are equalized. The corresponding normalized spatiotemporal equation reads

$$u_z = (i/2)(u_{xx} + u_{yy} + u_{tt}) = (i/2)(2u_r/r + u_{rr}), \quad (6)$$

where $r = \sqrt{x^2 + y^2 + t^2}$. By applying the transformation $u(r,z) = \phi(r,z)/r$, the problem is reduced to the one-dimensional diffraction equation $i\phi_z + \phi_{rr} = 0$. Here we focus on the following exact Airy-like solution of the three-dimensional problem:

$$u(r,z) = [g(r_0 - r, z) - g(r_0 + r, z)]/r, \quad (7)$$

where $g(r,z)$ is given by Eq. (4). Note that the numerator of Eq. (7) becomes zero for $r = 0$. The first terms of the expansion of Eq. (7) close to the origin are given by

$$u(r,z) \approx -2g_{r_0}(r_0,z) - g_{r_0r_0r_0}(r_0,z)(r^2/3), \quad (8)$$

where

$$u(r=0,z) = -2g_{r_0}(r_0,z) = -e^{i\Psi(r_0,z)}[(2\alpha + iz)\mathrm{Ai}(\xi(r_0,z)) + 2\mathrm{Ai}'(\xi(r_0,z))], \quad (9)$$

$g_{r_0r_0r_0}(r_0,z) = (1/2)e^{i\Psi(r_0,z)}[f_1(r_0,z)\mathrm{Ai}'(\xi(r_0,z)) + f_2(r_0,z)\mathrm{Ai}(\xi(r_0,z))]$, $\Psi(r,z) = (6\alpha^2 z - 6i\alpha(2r - z^2) + 6rz - z^3)/12$, $\xi(r,z) = -z^2/4 + i\alpha z + r$, $f_1(r,z) = 2(3\alpha^2 + 4i\alpha z + r - z^2)$, and $f_2(r,z) = 2\alpha^3 + 9i\alpha^2 z + 6\alpha(r - z^2) + 3irz - iz^3 + 2$. Equation (7) exhibits abruptly autofocusing dynamics [see Fig. 3]. However, since the energy is initially spread out on a three-dimensional ring, even higher intensity contrasts are attained; the maximum intensity that the Airy wave reaches during propagation is between 3 and 4 orders of magnitude larger than the original intensity. Other scenarios where the third dimension might be utilized include the use of two Airy pulses, the first one decelerating and the second one accelerating so that the waves simultaneously collide in space and time, or the use of appropriately chirped pulses. Such approaches are feasible even in the region of normal dispersion.

In conclusion, we have shown that families of two-dimensional and three-dimensional waves can autofocus in an abrupt fashion. We would like to point out that the general concept of autofocusing presented here is more general and, in principle, can be extended to other wave functions beyond Airy. However, the curved nondiffracting dynamics of Airy beams has several advantages, including enhanced autofocusing contrast and abruptness, especially in the case of long focal lengths. Other families of beams might also exist exhibiting abrupt autofocusing properties. In particular, we have investigated different wave configurations, the results of which will be presented elsewhere.

This work was partially supported by United States Air Force Office of Scientific Research (USAFOSR) grant no. FA9550-10-1-0561.

References

1. B. E. A. Saleh and M. C. Teich, *Fundamentals of Photonics*, 2nd ed. (Wiley, 2007).
2. A. E. Seigman, *Lasers* (University Science, 1986).
3. T. Juhasz, F. Loesel, R. Kurtz, C. Horvath, J. Bille, and G. Mourou, IEEE J. Sel. Top. Quantum Electron. **5**, 902 (1999).
4. K. M. Davis, K. Miura, N. Sugimoto, and K. Hirao, Opt. Lett. **21**, 1729 (1996).
5. M. Mlejnek, E. M. Wright, and J. V. Moloney, Opt. Lett. **23**, 382 (1998).
6. S. Tzortzakis, L. Bergé, A. Couairon, M. Franco, B. Prade, and A. Mysyrowicz, Phys. Rev. Lett. **86**, 5470 (2001).
7. G. S. He, in Vol. 53 of *Progress in Optics* (Elsevier, 2009), Chap. 4, pp. 201–292.
8. G. A. Siviloglou and D. N. Christodoulides, Opt. Lett. **32**, 979 (2007).
9. G. A. Siviloglou, J. Broky, A. Dogariu, and D. N. Christodoulides, Phys. Rev. Lett. **99**, 213901 (2007).
10. M. V. Berry and N. L. Balazs, Am. J. Phys. **47**, 264 (1979).
11. J. Baumgartl, T. Čižmár, M. Mazilu, V. C. Chan, A. E. Carruthers, B. A. Capron, W. McNeely, E. M. Wright, and K. Dholakia, Opt. Express **18**, 17130 (2010).